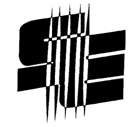

ISSN 1225-8024(Print)
ISSN 2288-8403(Online)

한국표면공학회지
J. Kor. Inst. Surf. Eng.
Vol. 48, No. 3, 2015.
http://dx.doi.org/10.5695/JKISE.2015.48.3.126

<연구논문>

Substrate Temperature Dependence of Microcrystalline Silicon Thin Films by Combinatorial CVD Deposition

Yeonwon Kim*

Division of Marine Engineering, Korea Maritime University, Busan 606-791, Korea

(Received June 22, 2015 ; revised June 25, 2015 ; accepted June 29, 2015)

Abstract

A high-pressure depletion method using plasma chemical vapor deposition (CVD) is often used to deposit hydrogenated microcrystalline silicon (μc-Si:H) films of a low defect density at a high deposition rate. To understand proper deposition conditions of μc-Si:H films for a high-pressure depletion method, Si films were deposited in a combinatorial way using a multi-hollow discharge plasma CVD method. In this paper the substrate temperature dependence of μc-Si:H film properties are demonstrated. The higher substrate temperature brings about the higher deposition rate, and the process window of device quality μc-Si:H films becomes wider until 200°C. This is attributed to competitive reactions between Si etching by H atoms and Si deposition.

Keywords : Microrystalline silicon, Temperature dependence, Chemical vapor deposition

1. Introduction

Tandem Si thin film solar cells are fabricated using amorphous silicon (a-Si:H) cells as the top cells and microcrystalline silicon (μc-Si:H) as the bottom cells, in order to realize high efficiency with low manufacturing cost[1]. One of the important issues of μc-Si:H film deposition is a low film defect density at a high rate above 2.0 nm/s. Recently, a deposition in high pressure depletion regime using plasma enhanced chemical vapor deposition (CVD) has been proposed as a deposition method leading to much higher growth rates while preserving acceptable film quality[2-6]. It has been reported that deposition in high pressure depletion regime has been successfully used to deposit μc-Si:H films of 9×10^{15} cm^{-3} in defect density at a rate of 8 nm/s with multi-hollow CVD method[7-10]. However, in spite of such success it is still difficult to deposit μc-Si:H films of a low density at a high deposition rate on a large substrate in industry because of a narrow process window. Especially deposition mechanism bringing about high quality films has not been fully clarified yet.

In μc-Si:H film deposition, SiH_3 radicals and H atoms impinging to surface of films play key roles [11,12]. A high flux of H atoms causes local heating through hydrogen-exchange reactions on surface of films. Such local heating enhances the surface diffusion of SiH_3, being the predominant deposition precursor. SiH_3 radicals on surface react at energetically favorable sites, leading to the crystalline nucleation. After the nucleation, epitaxial-like crystal growth takes place with enhanced surface diffusion of SiH_3 radicals[13,14]. For the high pressure depletion method, a wider process window should be realized based on the knowledge of deposition mechanism in detail[15]. Optimization of μc-Si:H solar cells requires deeper understanding of the material properties in the high depletion regime, especially the process window of high quality microcrystalline films determined by etching by H[16,17] and surface diffusion of deposition radicals[18]. To gain further insight into the deposition mechanism, we have applied a multi-hollow discharge plasma chemical vapor deposition (CVD) method by which contribution of SiH_3 radicals and H atoms to deposition as well as their flux ratio varies with the distance between the substrates and

*Corresponding Author : Yeonwon Kim
Division of Marine Engineering, Korea Maritime University
E-mail : k.yeonwon@gmail.com

the discharges[19-22]. In this article, we present the experimental results obtained under the high pressure depletion conditions and, based on the results we discuss relation between the process window and substrate temperature.

2. Experimental Details

Figure 1 shows a schematic diagram of the multi-hollow discharge plasma CVD reactor[23]. Multi-hollow electrodes had 24 holes of 5mm in diameter, in which the discharges were sustained. VHF power of 180 W (60 MHz) was applied between one powered electrode and a pair of grounded electrodes to generate plasma. SiH_4 diluted with H_2 was supplied to the reactor. The silane dilution ratio R= $[SiH_4]/([H_2]+[SiH_4])$ were kept at 0.997. The total pressure was 2 Torr. The substrate holder was set vertically on the powered electrode. This combinatorial study such as vertical deposition makes it possible to obtain more information on spatial distribution of deposition radicals, etching precursors and film properties with single experiment. The substrate temperatures (T_s) were varied from room temperature (RT) to 350°C. Crystalline volume fraction and crystalline orientation were determined with a Raman spectroscope (Jasco, NRS-3100) and X-ray diffraction (XRD) spectrometer (Bruker, D8 DISCOVER), respectively. Deposition rate was obtained as film thickness divided by deposition time. Defect density was measured with an electron spin resonance (ESR) spectrometer (Bruker, EMX)[24,25].

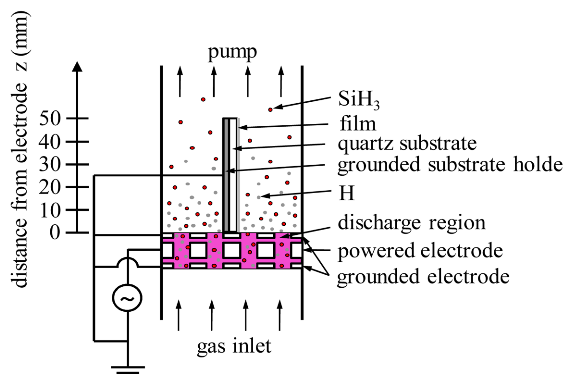

Fig. 1. Schematic diagram of multi-hollow discharge plasma CVD reactor.

3. Results and Discussion

Figure 2 shows two-dimensional scanned images of deposited films s a parameter of substrate temperatures (T_s), which is obtained with generally used optical scanner. Black dark films near the etched regions (no-film region) shows high roughness about 10 nm with atomic force microscope (AFM), whereas brown films are lower roughness under 10nm. this indicate that near-discharge region is more affected by radical etch compared to far-discharge region. The no-film region is found in all temperature range and the region decreases with increasing (T_s). These results show that μc-Si:H deposition is decided by competitive reactions between etching by H atoms and Si deposition, and the contributions of etching and deposition are effected by T_s[26].

Figure 3 shows that their deposition rate and crystal volume fraction (X_c) from near-discharge region to far-discharge region. The deposition rated is measured with cross section image of scanning electron microscope (SEM), and crystalline volume fraction (X_c) is deduced from the integrated intensity ratio, $X_c = (I_{520} + I_{500})/(I_{520} + I_{500} + I_{480})$, by de-convolution of the Raman spectra into three characteristic Raman peaks positioned at 480, 500 and 520 cm^{-1} [27]. The deposition rate decreases exponentially as shown in Fig. 3(a), because SiH_3 density, which is the main deposition precursor for high-quality films, decreases exponentially with z due to their loss on the surfaces[28-30]. In Fig. 3(b) we can clearly identify the crystallized region and the amorphous region. White dotted lines shown in Fig. 2 indicate the boundary between these two regions. The crystalline volume fraction is high near the discharge region and drops sharply in a transition region around z = 20 - 40 mm.

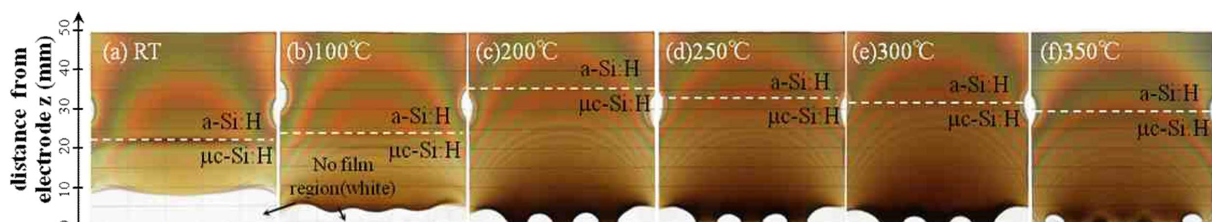

Fig. 2 Images of films prepared by multi-hollow discharge plasma CVD method as a parameter of substrate temperature, T_s = RT-350°C,180 W (60 MHz), R = 0.997, 2Torr.

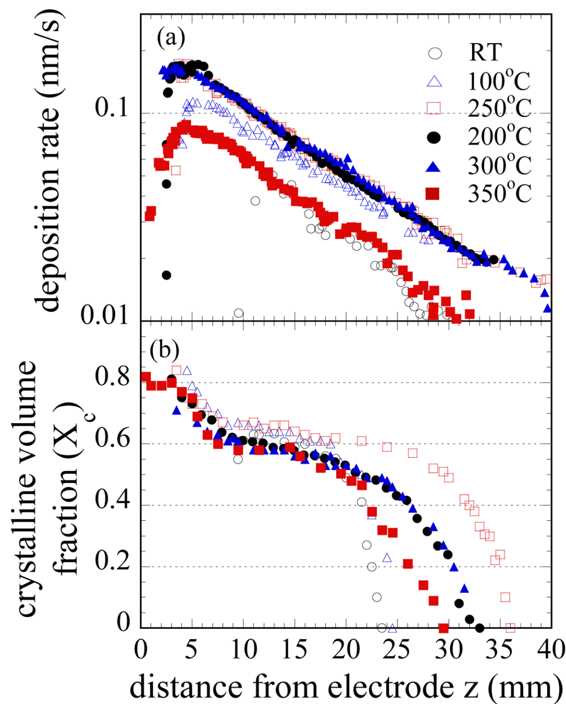

Fig. 3. Deposition rate (a) and crystalline volume fraction (X_c) (b) as a function of a distance from electrode.

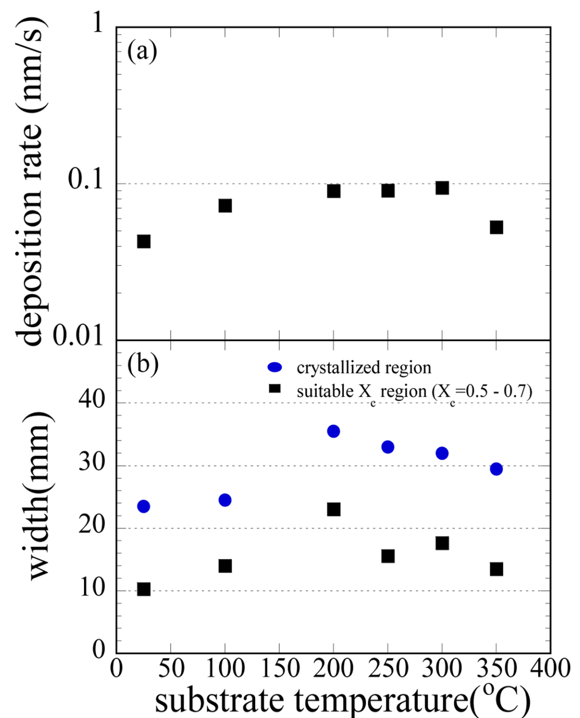

Fig. 4. Substrate temperature (T_s) dependence of deposition rate (a) and width of crystallized region (b).

These results suggest a flux ratio of H to SiH_3 (H/SiH_3) radicals is high near the discharge region and decreases with z, because a high flux ratio is needed for μc-Si:H film deposition. The area of micro-crystalline Si region increases with Ts due to high surface diffusion rate of deposition radicals[31]. These results show that the process window of μc-Si:H films becomes wider for the higher substrate temperature due to the lower Si etching rate and the longer surface migration length of Si containing radicals.

To investigate the process window of μc-Si:H film, we plotted width of $X_c = 0.5 - 07$ region with T_s and their deposition rate. It is considered that grain boundary of crystalline silicon is well passivated with amorphous silicon for range of $X_c = 0.5 - 07$ range, whereas the high crystallity film have too much of grain boundary defect. Fig. 4(a) shows that deposition rate of $X_c = 0.5 - 0.7$ region as a function of Ts. It increases with Ts up to 200°C, nearly constant for 200 - 300°C, and decreases for T_s of 350°C. Fig. 4(b) shows the width of crystallized region ($X_c > 0$) and that of $X_c = 0.5 - 0.7$. They increase up to T_s of 200°C, then decrease to T_s of 300°C. This results represent that the condition of 200°C shows high deposition rate with wide process window.

To obtain more information on above specific region ($X_c = 0.5 - 07$) of the film structure, we evaluated crystalline orientation and grain size from XRD spectra using the peak intensity ratio of the (220)/(111) and peak width from the Scherrer's equation[32], respectively. The columnar structure of (220) orientated growth and large grain size are more favorable when the film used as solar cell due to their lower grain boundary defect. Fig. 5(a) shows the T_s dependence of the film orientation in X_c=0.5-0.7 film region. The random growth of (111) orientated μc-Si:H films are obtained preferentially at relatively low T_s of 100°C, and that the preferential crystal orientation changes from (111) to (220) at T_s of 200°C and maintain the constant value over T_s of 200°C. The (200) crystallite size increases slightly with T_s as shown in Fig. 5 (b).

Figure 6 shows T_s dependence of dangling-bond defect density Ns of films of the $X_c = 0.5$-0.7 region. For T_s = 100°C, it shows the value of 6.24×10^{16} cm^{-3} due to not enough surface migration of Si and H radicals on the surface resulting in high dangling bond defect, and it decreases significantly with T_s down to 6.26×10^{15} cm^{-3} until T_s 300°C due to the passivation of dangling-bond resulting from surface migration with enough substrate temperature. However, Over 300 °C, it is considered that too high substrate temperature induce the dangling bond defect by breaking H bond in film surface.

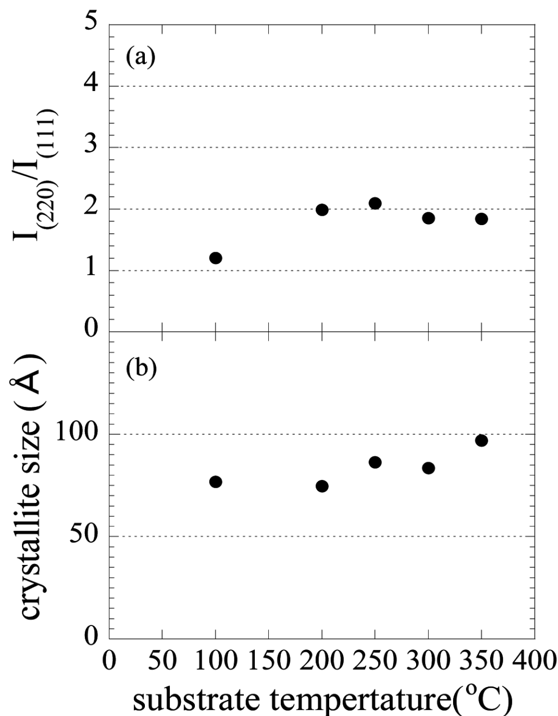

Fig. 5. Substrate temperature (T_s) dependence of crystal orientation ratio of (220) to (111) (a) and (220) crystallite size (b).

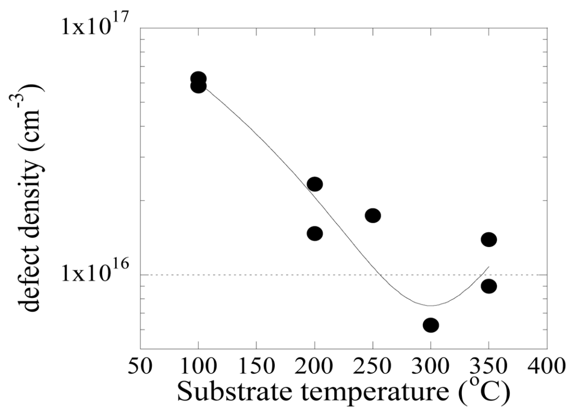

Fig. 6. Substrate temperature (T_s) dependence of μc-Si film (X_c = 0.5 - 0.7).

4. Conclusions

The combinatorial technique using the multi-hollow discharge plasma CVD method have been used to investigate the effects of substrate temperature on the μc-Si:H film growth. No film is deposited near the discharge region at low substrate temperature from RT to 100°C, whereas the area of no film region decreases with increasing the substrate temperature. This is attributed to competitive reactions between Si etching by H atoms and Si deposition. The area of microcrystalline Si region increases with the substrate temperature due to high surface diffusion rate. These results show that the process window of μc-Si:H films becomes wider for the higher substrate temperature due to two reasons: 1) the lower Si etching rate and 2) the longer surface migration length of Si containing radicals. The defect density has a high value of 6.24 × 10^{16} cm^{-3} for T_s = 100°C, it decreases significantly with T_s down to 6.26 × 10^{15} cm^{-3} for T_s=300°C.

References

1. J. Meir, S. Dubail, R. Fluckiger, H. Keppner, and A. Shah : Proc. 1st WCPEC (1994) 409.
2. Y. Sobajima, T. Higuchi, J. Chantana, T. Toyama, C. 0Sada, A. Matsuda, and H. Okamoto : Phys. Status Solidi C 7 (2010) 521.
3. S. Nunomura, I. Yoshida, M. Kondo : Appl. Phys. Lett. 94 (2009) 071502.
4. Y. Sobajima M. Nishino, T. Fukumori, T. Higuchi, S. Nakano, T. Toyama, H. Okamoto : Sol. Energy Mater. Sol. Cell 93 (2009) 980.
5. M. Kondo, M. Fukawa, L. Guo, A. Matsuda : J. Non- Cryst. Solids 84 (2000) 266.
6. S. Klein, F. Finger, R. Carius, M. Stutzmann : J. Appl. Phys. 98 (2005) 024905.
7. L. Guo, M. Kondo, M. Fukawa, K. Saitoh, and A. Matsuda : Jpn. J. Appl. Phys. 37 (1998) L1116.
8. M. Kondo, M. Fukawa, L. Guo, and A. Matsuda : J. Non-Cryst. Solids 266–269 (2000) 84.
9. A. Matsuda : Jpn. J. Appl. Phys. 43 (2004) 7909.
10. Y. Sobajima, T. Higuchi, J. Chantana, T. Toyama, C. Sada, A. Matsuda, and H. Okamoto : Physica Status Solidi C 7 (2010) 521.
11. G. Dingemans, M. N. van den Donker, D. Hrunski, A. Gordijin, W. M. M. Kessels, and M. C. M. van de Sanden : Appl. Phys. Lett. 93 (2008) 111914.
12. A. A. Howling, R. Sobbia, and Ch. Hollenstein : J. Vac. Sci. Technol. A 28 (2010) 989.
13. A. Matsuda: : J. Non-Cryst. Solids 59–60 (1983) 767.
14. A. Matsuda : Thin Solid Films 337 (1999) 1.
15. J. K. Rath, A. D. Verkerk, Y. Liu, M. Brinza, W. J. Goedheer, and R. I. E. Schropp : Mater. Sci. Eng. B 159–160 (2009) 38.
16. X. R. Duan, H. Lange, A. Meyer-Plath : Plasma Sources Sci. Technol.12 (2003) 554.
17. P. Kae-Nune, J. Perrin, J. Jolly, and J. Guillon : Surf. Sci. 360 (1996) L495.
18. W. Beyer : Sol. Energy Mater. Sol. Cells 78, (2003) 235.
19. K. Koga, T. Inoue, K. Bando, S. Iwashita, M. Shiratani, and Y. Watanabe : Jpn. J. Appl. Phys. 44 (2005) L1430.

20. W. M. Nakamura, H. Miyahara, H. Sato, H. Matsuzaki, K. Koga, and M. Shiratani : IEEE Trans. Plasma Sci. 36 (2008) 888.
21. W. M. Nakamura, H. Miyahara, K. Koga, and M. Shiratani : J. Phys.: Conf. Ser. 100 (2008) 082018.
22. H. Sato, Y. Kawashima, M. Tanaka, K. Koga, W. M. Nakamura, and M. Shiratani : J. Plasma Fusion Res. SERIES 8 (2009) 1435.
23. K. Koga, T. Inoue, K. Bando, S. Iwashita, M. Shiratani, and Y. Watanabe : Jpn. J. Appl. Phys. 44, (2005) L1430.
24. M. H. Brodsky, R.S. Title : Phys. Rev. Lett. 23 (1969) 581.
25. S. T. Pantelides : Phys. Rev. Lett. 57, (1986) 2979.
26. J. Abrefah, D.R. Olander : Surf. Science. 209, (1989) 291.
27. L. Houben, M. Luysberg, P. Hapke, R. Carius, F. Finger and H. Wagner : Philos. Mag. A 77 (1998) 1447.
28. Itanashi, N. Nishikawa, M. Magane, S. Naito, T. Goto, A. Matsuda, C. Yamada, and E. Hirota : Jpn. J. Appl. Phys. 29 (1990) L505.
29. J. Perrin, M. Shiratani, P. Kae-Nune, H. Videlot, and J. Guillon : J. Vac. Sci. Technol. A, Vac. Surf. Films 16 (1998) 278.
30. O. Vetterl, F. Finger, R. Carius, P. Hapke, L. Houben, O. Kluth, A. Lambertz, A. Mück, B. Rech, and H. Wagner : Sol. Energy Mater. Sol. Cells 62 (2003) 97.
31. P. C. P. Bronsveld, J. K. Rath, and R. E. I. Schropp, et al., : Appl. Phys. Lett. 89 (2006) 051922.
32. S. Vepřek, F.-A. Sarott and M. Rückschloß, J. Non-Cryst. Solids 137&138 (1991) 733.